Archives of Hydro-Engineering and Environmental Mechanics
Vol. 59 (2012), No. 3–4, pp. 137–153
DOI: 10.2478/heem-2013-0008-y

VERSITA

On Flow-Altering Countermeasures for Scour at Vertical-Wall Abutment

Alessio Radice[*], **Oskars Lauva**[**]

[*] Assistant Professor, Dept. I.I.A.R., Politecnico di Milano, Piazza Leonardo da Vinci, 32, 20133 Milano, Italy, Corresponding author, E-mail: alessio.radice@polimi.it

[**] M.Sc. student in Heat, Gas and Water Technology, Faculty of Civil Engineering, Riga Technical University, Azenes street 16/20, Riga, LV-1048, Latvia

(Received April 03, 2012; revised October 10, 2012)

Abstract

Results are presented for clear-water scour experiments at a vertical-wall abutment where the obstacle was modified with slots or roughening elements as flow-altering countermeasures against the erosion process. The laboratory campaign comprehended an initial experiment with an unprotected obstacle, two experiments with slots above and beneath the non-scoured bed level, respectively, and one experiment with a roughened abutment. The repeatability of the experiments was checked and found satisfactory. The measured data set consisted of (i) scour depth with time; (ii) geometry of the erosion hole; and (iii) sediment motion pattern at several evolution stages of the process. A novel feature of the work was the attempt to combine evidence on the scour depth and that on sediment motion so as to shed light on the mechanism of scour reduction by the countermeasures tested. It is argued that this strategy might furnish guidelines for future extensive investigations of scour countermeasures, aimed at finding optimal design solutions.

Key words: local scour, abutment, process dynamics, flow-altering countermeasures, sediment transport

Notation

b – abutment length,
B – duct width,
C – areal concentration of sediments in motion,
d – sediment size,
ds – maximum scour depth,
g – acceleration due to gravity,
h – flow height,
Q – water discharge,
Q_c – threshold value of water discharge,

q_s – sediment transport rate per unit width (component along the flow direction),
$\boldsymbol{q}_s$ – sediment transport rate per unit width (vector),
T – time of experiment,
$\boldsymbol{v}_s$ – sediment velocity (vector),
$W_{downstream}$ – volume of the scour hole downstream of the abutment,
$W_{total} = W_{upstream} + W_{downstream}$,
$W_{upstream}$ – volume of the scour hole upstream of the abutment,
x – longitudinal coordinate,
y – transverse coordinate,
z – elevation above non-scoured bed level,
$\Delta = (\rho_g - \rho)/\rho$,
ϕ – Shields number,
ϕ_c – threshold value of the Shields number,
Φ – dimensionless sediment transport rate per unit width,
ρ – water density,
ρ_g – sediment density.

1. Introduction

One of the major causes of bridge failure or collapse is local scour, which is due to a three-dimensional, vortical flow system induced by the structures' interception of the river flow. In recent years, extensive research (see, for reviews, Melville and Coleman 2000, Lagasse et al 2001) has been aimed at finding methods to efficiently reduce the expected scour levels at both piers and abutments, the latter being within the scope of this work.

Scour countermeasures are typically divided into (i) bed-armoring devices and (ii) flow-altering devices. The former increase the resistance of the river bed and include riprap blocks or similar tools (recent examples for abutments include Melville et al 2006a and 2006b, Korkut et al 2007, Cardoso and Fael 2009, Sui et al 2010). The latter (examples for pier protection are given when they are not available for abutments) reduce the strength of the turbulent flow field and include collars and/or slots (e.g., Dargahi 1990, Chiew 1992, Kumar et al 1999, Zarrati et al 2004, Heidarpour et al 2010), vanes (e.g., Johnson et al 2001, Li et al 2006), sacrificial piles (Melville and Hadfield 1999, Haque et al 2007), structure threading (Dey et al 2006), and sills (e.g., Chiew and Lim 2003, Grimaldi et al 2009). In some cases, combinations of bed-armoring and flow-altering devices have been proposed (e.g., Mashahir et al 2010, Zarrati et al 2010). In general, studies on scour countermeasures have involved extensive laboratory campaigns aimed at finding configurations for which sufficient reductions in the scour depth could be obtained.

The experiments documented in this manuscript dealt with flow-altering countermeasures for bridge abutments, a field scarcely covered in the previous literature.

A distinctive feature of this study was the attention paid to the mechanisms of the scour process at protected obstacles. The purpose was not to propose optimal engineering solutions, which would have required much more extensive experimental campaigns. The experiments presented here were rather meant to clarify the functioning of selected devices and thus to provide guidance for further experimental campaigns.

2. Experiments

A 5.8 m long, pressurized, transparent duct with a rectangular cross section (width $B = 40$ cm and height $h = 16$ cm) was used for the experimental tests. The last part of the duct was a 2 m long recess section filled with loose sediments. These were simulated with uniform circular PVC cylinders, which were used instead of spheres because this is the shape in which PVC particles are typically produced as semi-manufactured materials for several industrial applications. The particle shape should have only a marginal influence on the results documented in the following. The characteristic size of the grains, however, was determined as the diameter of a sphere having the same volume as the PVC cylinder. This size was 3.6 mm, and in the following will be referred to as d. The specific gravity of the sediment particles was $\Delta = (\rho_g - \rho)/\rho = 0.43$, with ρ_g and ρ being the densities of PVC and water, respectively. The same sediments were glued onto the bottom of the remaining part of the duct to ensure homogeneity of the bed roughness.

The vertical-wall abutment model used here was a plate of length $b = 100$ mm. Given the width of the experimental channel, the contraction ratio resulted as $b/B = 0.25$. The experiments documented in the following might thus be affected by flow constriction, but at least two considerations could be made in this respect: (i) the effect of the contraction ratio for vertical-wall abutments was specifically addressed by Ballio et al (2009), who found that the scour expectable for $b/B = 0.25$ was less than 1.10 times that for $b/B \leq 0.10$ (condition considered unaffected by contraction), except for the very beginning of the experiments (corresponding to $ds/bh^{0.5} \leq 1$, with ds as the maximum scour depth); (ii) however, the study presented here involved the comparison of scour depths obtained for abutments of the same length, so the contraction ratio was always kept the same.

The reference system used throughout the analysis involved the x axis aligned with the main flow, the y axis from the left to the right wall of the duct, and the z axis as elevation above the non-scoured bed level. The plan coordinates of the abutment nose were set at $x = 1,000$ mm, $y = 100$ mm.

As mentioned, only flow-altering countermeasures are within the scope of this study (a very preliminary documentation for a bed-armoring device applied to the present abutment can be found in Radice 2010). Therefore, the experimental campaign comprehended the following four configurations: (U) unprotected abutment (that was actually a repetition of an experiment performed by Radice et al 2009b and further analyzed by Radice et al 2010); (SA) abutment with a slot above the non-scoured bed

level; (SB) abutment with a slot beneath the non-scoured bed level; (R) roughened abutment. Fig. 1 shows a sketch of the four abutments. In both SA and SB tests, the dimension of the slot was 30×80 mm. The position of the slot was such that the distance between the non-scoured bed level and the edge of the slot was 40 mm in both cases (i.e. the bottom edge for SA and the top edge for SB). In the R test, the size of the roughening elements and the spacing between them were 10 and 30 mm, respectively.

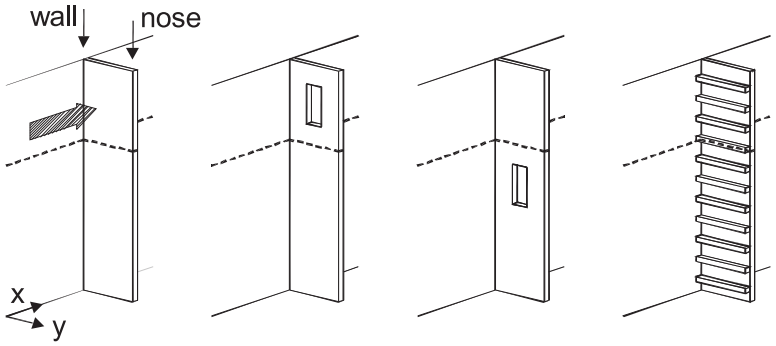

Fig. 1. The abutments used in the four experiments: unprotected (U), with slot above bed level (SA), with slot beneath bed level (SB), roughened (R). All abutments were placed at the left side of the duct. The dashed line represents the trace of the non-scoured sediment level. The flow direction, coordinate system and measuring points for the scour depth indicated in the sketch for the U abutment are valid also for the others

The threshold water discharge for incipient particle motion was experimentally determined by Radice and Ballio (2008). It is well known that the definition of the critical condition is not straightforward (see, for example, Buffington and Montgomery 1997). Radice and Ballio (2008) identified the condition of incipient particle motion with $\Phi = q_s / \left(g \times \Delta \times d^3\right)^{0.5} = 6 \times 10^{-5}$, where Φ and q_s are dimensionless and dimensional sediment transport rates per unit width, respectively, and g is the acceleration due to gravity. The chosen sediment transport rate corresponds to $\phi/\phi_c = 1.01$ (ϕ is the Shields (1936) number and ϕ_c is its threshold value) if the equation of Meyer-Peter and Müller (1948) and $\phi_c = 0.04$ are used. The water discharge corresponding to the critical conditions was $Q_c = 19.0$ l/s.

The scour experiments documented in the following were carried out with a discharge $Q = 18.5$ l/s and were thus clear-water, near-critical scour experiments. Before the start of a test, the duct was slowly filled with water, and a discharge lower than 7.0 l/s was established to prevent anticipated scour. The discharge was then progressively increased up to the desired value (the transient was monitored through a magnetic flowmeter and typically lasted less than 1 minute).

Each test was performed twice, with the first and second runs being devoted to the measurement of scour and sediment motion, respectively. During the first runs, the scour depth was frequently measured upstream of the abutment nose (nose measuring point at $x = 990$ mm, $y = 100$ mm) and near the duct wall (wall measuring point at $x = 990$ mm, $y = 0$). For the former measurement, a laser sensor positioned on a support above the duct lid and capable of measuring through the lid was used. The measurement at the wall point was instead made with a ruler attached to the lateral wall of the duct. At some evolution stages, the discharge was decreased to stop the process temporarily, and surveys were made of several transverse and longitudinal sections of the scour hole. A temporary stop and restart of the experiment did not cause significant distortions to the measured temporal trend of the scour depth even though the 'freezed' geometry of the scour hole may have been slightly different from that for the phenomenon in progress.

During the second runs, the motion of the sediments on the bottom of the hole was filmed at several evolution stages, using a motion camera with a resolution of $1,024 \times 800$ pixel and the frame rate set to 50 Hz. In addition, scour depth values were taken to check test repeatability in comparison with the other runs. The experiments were filmed from above, and the planar focus area was approximately 250×200 mm^2. Sediment motion was measured by the method of Radice et al (2006). The sediment kinematics was quantified through the areal concentration of moving sediments C and the vector particle velocity $\boldsymbol{v}_s$, the two quantities being related to the vector solid discharge per unit width ($\boldsymbol{q}_s$) as $\boldsymbol{q}_s = C \times \boldsymbol{v}_s \times d$. The concentration of moving particles was measured through image subtraction and following proper image filter. The sediment velocity was measured by Particle Image Velocimetry, using interrogation areas with a side of 2 cm and a maximum measurable velocity of 20 cm/s. Since the experiments were filmed from above and no projection of velocity was made, the measurement did not include the vertical motion of the particles.

The experimental configuration used here was different from those typically applied for scour analyses for two reasons, namely (i) the use of lightweight material and (ii) the covered flow condition. Radice et al (2009a and 2009b) addressed these issues in detail. The key points of the referenced discussions are sketched here. The low density of the sediments is accounted for in the estimation of the threshold conditions for incipient particle motion; thus, the experiments documented here were run at nearly threshold conditions like most of the literature ones with natural sand. The pressure flow changes the features of the near-obstacle flow field because a second principal vortex is created by the separation of the boundary layer at the duct lid, but interference between the two principal vortices progressively decreases because the bottom one sinks into the scour hole. Another difference is that the rise of the water surface upstream of the pier is prevented, but such rise may be expected to be modest for the low Froude number used here. Finally, Radice et al (2009b) presented a comparison between two abutment scour experiments, in which the runs were for natural sediments with a free surface and lightweight sediments with covered flow, respec-

tively. Once a proper dimensionless comparison was made, the difference between the two experiments turned out to be a decreasing function of the run time and was lower than 15% for the advanced stages of the process, corresponding to a range typically considered more than acceptable for scour predictions. It is therefore proposed here that the results shown, though strictly representative of scour in covered flow, may have equal applicability for scour with a free surface. The reader is redirected to the referenced works for further support to the last statement.

3. Results

3.1. Scour Depth

The temporal evolution of the scour depth at the two measuring points upstream of the abutment is depicted in Fig. 2 for all the experiments performed. For the unprotected abutment (U) the scour depth was initially larger at the nose, but it prevailed at the wall for $T > 4 \times 10^3$ s. The experiment, when compared with the one performed by Radice et al (2009b) (not shown here), proved a good repeatability of the process. For the evaluation of the performance of the tested countermeasures, the scour trends at the abutment nose and at the duct wall were considered separately. In general, none of the countermeasures caused an evident variation of the scour trend at the abutment nose. However, the devices changed the time evolution of the scour depth at the lateral wall. This location deserves attention because it was the position of the maximum scour depth in the U test and, moreover, the scour at the junction between the wall and the abutment would, in a real situation, affect the stability of the bank. During the SA experiment (Fig. 2a) the slot reduced the scour depth throughout the entire duration of the run, with greater (and significant) effect obtained for time $T > 10^3$ s. It was hypothesized that the beneficial effect of the slot in the advanced stages of the process was mainly related to the interception of the downflow in front of the abutment. The SB test presented (Fig. 2b) a different behavior, with the scour depth at the wall growing very rapidly as soon as the slot had been exposed $ds > 40$ mm). After a hole of around 120 mm had been scoured (that is, when the bottom of the scour hole had approached the bottom of the slot), the trends for U and SB tests tended to converge, and in the final part of the experiment ($T > 4 \times 10^3$ s) the slot appeared to have negligible effect. This finding supported the interpretation that at the beginning of the process the slot acted as a preferential way for the sediments to be conveyed away, whereas in the final stages this could not happen because the size of the slot was small in comparison with that of the scour hole and the bottom of the slot was much above the bottom of the hole. Finally, during the R test (Fig. 2c) the scour trend at the wall was initially close to that for the U test, but a reduction of scour could be obtained for $T > 800$ s. Thus, the roughening elements could not alter the flow field in the beginning of the scour process, but an effective change of the flow pattern was induced in the subsequent stages.

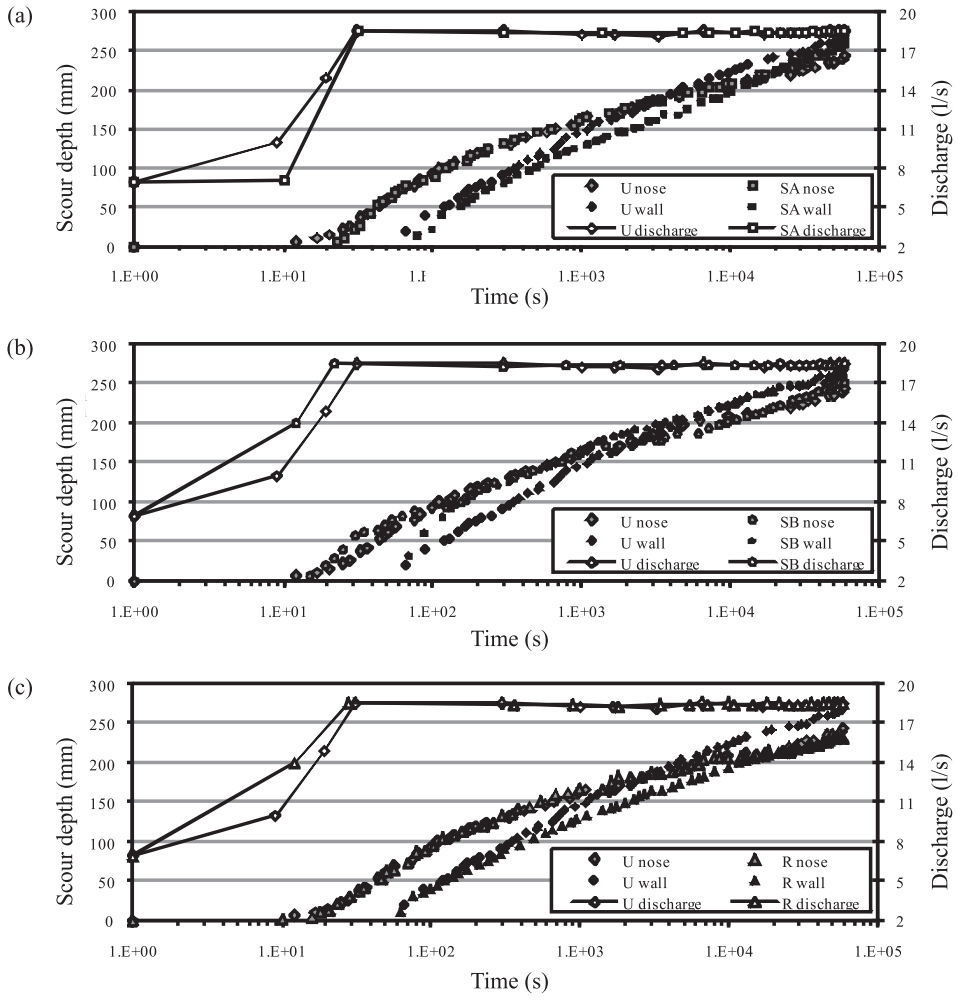

Fig. 2. Time evolution of the scour depth at the nose and wall measuring points: trend for the unprotected abutment compared with those for the protected ones: (a) SA, (b) SB, (c) R

Fig. 3 depicts the transverse section of the scour hole 10 mm upstream of the abutment face and the longitudinal section 10 mm distant from the wall, as surveyed at different times during all the experiments. The plots obviously confirm what is mentioned above with reference to the scour trends at the nose and wall points. In addition, it is worth noting that the SB test presented largest scour depths in the downstream portion of the scour hole, presumably due to a jet-like flow passing through the slot and impinging on the sediment bed.

The surveys of the transverse sections of the scour hole were used to compute its volume. The total volume of the hole (W_{total} henceforth) was split into the portions upstream of the abutment (for $x = 700 - 1,000$ mm, $W_{upstream}$) and downstream of the abutment (for $x = 1,000 - 1,500$ mm, $W_{downstream}$). The temporal evolution of the scoured volumes is depicted in Fig. 4, from which it can be seen that the countermeasures, though reducing the scour depth in the proximity of the obstacle, did not always reduce the volume of the scour depth. This result suggests that the flow field was distorted and deviated away from the abutment, but kept a scouring potential that developed elsewhere. Such a conclusion is in qualitative agreement with previous literature findings (e.g., Johnson et al 2001, Li et al 2006).

Some characteristic values of the scour depth and relative percentage reduction are reported in Tab. 1 for a general evaluation of countermeasure performance. A relatively small effect of the scour countermeasures on scour at the nose is represented by percentages, which are usually lower than 5% in absolute value. The poor performance of the SB configuration is also shown. Among the SA and the R configuration, the latter performed better, with scour reductions at the duct wall of around 15% in the advanced stages of the process. A similar analysis for the scoured volumes (see Tab. 2) showed that in most cases the reduction was negative, that is, the hole volume was larger in a protected test than in the unprotected one. For example, the R configuration induced the previously documented reduction for the wall point but involved an increase in the scour volume of around 5% in the final stage of the experiment. In other words, it seemed that an increase in the hole volume would be the price to pay for a reduction in the scour depth at the wall point. In this respect, it may be argued that focusing attention on the region closest to the abutment or on the global scour volume implies different perspectives, that is, the local stability of the obstacle or the amount of sediment leaving the river reach may be considered more or less important depending on various circumstances.

The obtained reductions in the scour depth were compared with values documented in the literature. For example, Chiew (1992) used slots as protections for circular piers and obtained scour reductions of up to 30%, but only using slots with a height equal to the water depth. Actually, it may be argued that piers with long slots tend to become similar to separate piles (which have also been proposed as scour countermeasures, e.g., Vittal el al 1994). However, for ratios of the slot height to the pier width similar to those used in the present study, Chiew (1992) obtained scour reductions similar to those found here. Furthermore, the roughened abutment con-

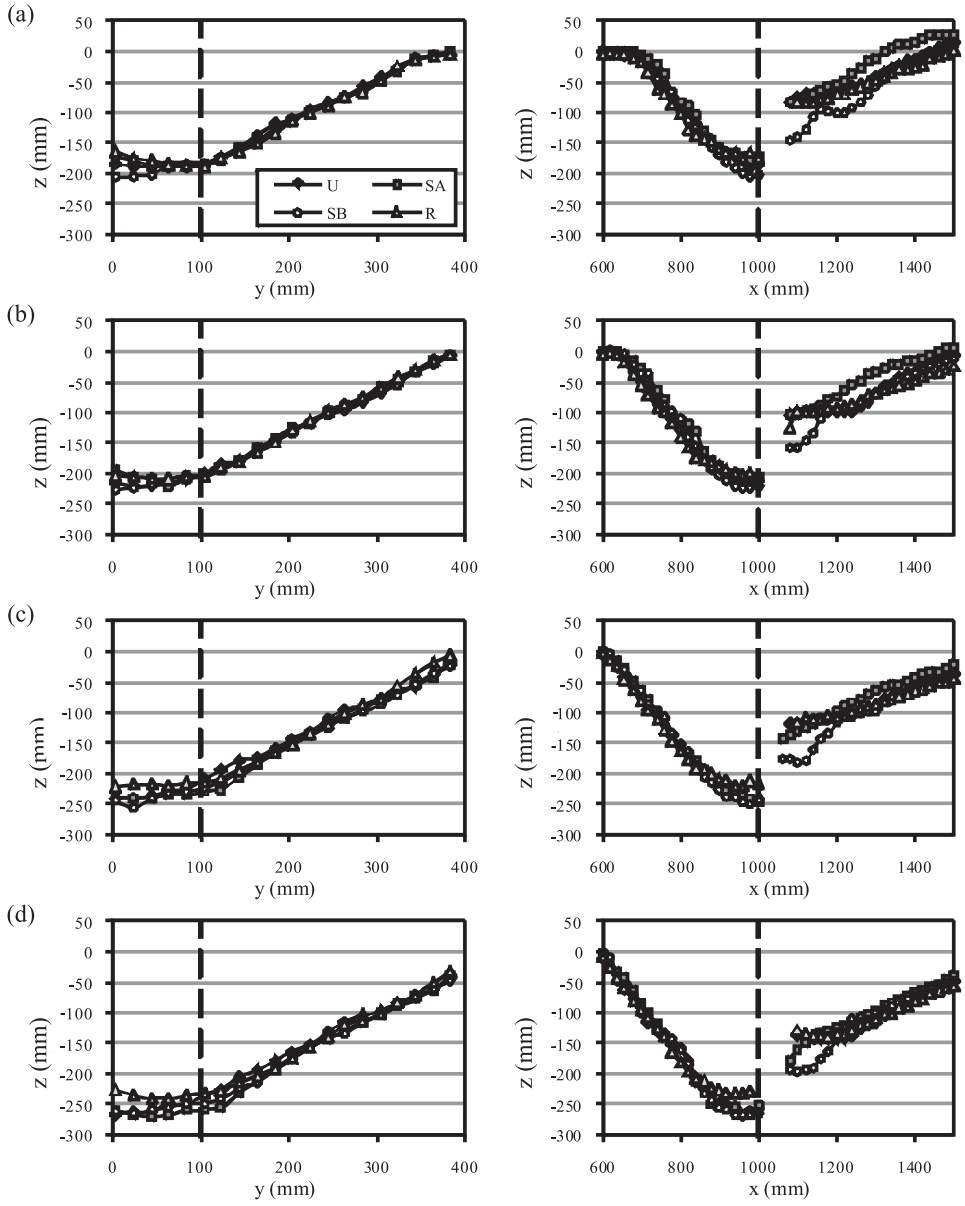

Fig. 3. Geometry of the scour hole represented through the transverse section 10 mm upstream of the abutment (left) and the longitudinal section 10 mm away from the lateral wall of the duct (right). Experimental times of survey: (a) 3,600 s; (b) 10,800 s; (c) 25,200 s; (d) 57,600 s. Dashed lines identify the vertical-wall abutment

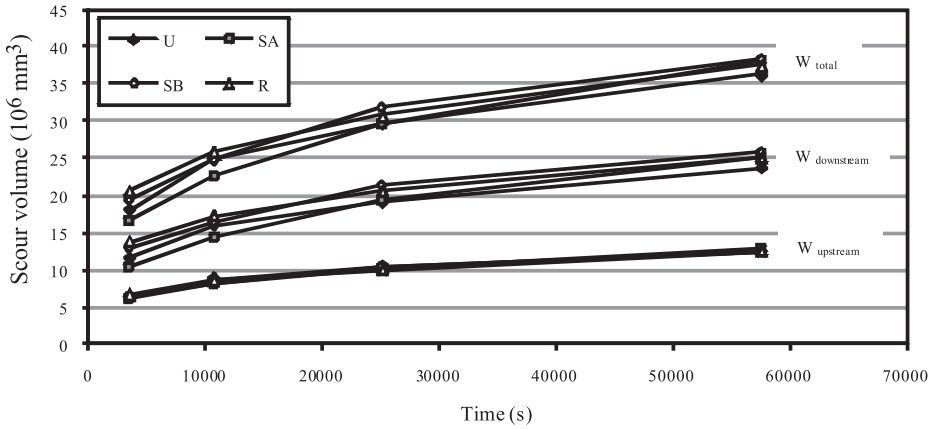

Fig. 4. Temporal evolution of the scoured volume for the experimental tests. $W_{upstream}$ and $W_{downstream}$ represent the volumes of the portions of the hole upstream and downstream of the abutment, respectively. W_{total} is the sum of the previous two contributions

Table 1. Scour depths (mm) and scour reduction (%) obtained in the tests with the protected abutment in comparison with the unprotected one

Time		180 s	3,600 s	10,800 s	25,200 s	57,600 s
Test U	Scour nose	115	193	209	219	245
	Scour wall	74	195	223	246	269
Test SA	Scour nose	115	188	209	230	261
	Scour wall	58	168	198	235	258
	% reduction nose	0.0	2.6	0.0	−5.0	−6.5
	% reduction wall	21.6	13.8	11.2	4.5	4.1
Test SB	Scour nose	108	183	204	225	251
	Scour wall	104	200	223	246	261
	% reduction nose	6.1	5.2	2.4	−2.7	−2.4
	% reduction wall	−40.5	−2.6	0.0	0.0	3.0
Test R	Scour nose	118	188	199	217	232
	Scour wall	66	165	180	211	231
	% reduction nose	−2.6	2.6	4.8	0.9	5.3
	% reduction wall	10.8	15.4	19.3	14.2	14.1

sidered here was similar to the threaded pier proposed by Dey et al (2006). They obtained scour reductions of up to 40%, but the ratio of the thread size to the obstacle size was much larger than the analogous one for the roughening elements used here (0.33 instead of 0.10), and indeed the authors acknowledged that it was quite large compared with technical possibilities.

Table 2. Scour volumes (10^6 mm^3) and relative reduction (%) obtained in the tests with protected abutment in comparison with the unprotected one

Time		3,600 s	10,800 s	25,200 s	57,600 s
Test U	$W_{upstream}$	6.3	8.8	10.5	12.5
	$W_{downstream}$	11.7	16.1	19.2	23.8
	W_{total}	18.1	24.9	29.7	36.3
Test SA	$W_{upstream}$	6.2	8.2	10.2	13.0
	$W_{downstream}$	10.5	14.5	19.4	25.1
	W_{total}	16.7	22.7	29.6	38.1
	% reduction upstream	2.1	7.2	2.9	−4.3
	% reduction downstream	10.6	9.8	−0.8	−5.5
	% reduction total	7.6	8.9	0.5	−5.1
Test SB	$W_{upstream}$	6.6	8.4	10.4	12.4
	$W_{downstream}$	12.9	16.5	21.5	26.0
	W_{total}	19.6	24.9	31.9	38.4
	% reduction upstream	−4.4	4.6	0.8	0.4
	% reduction downstream	−10.2	−2.6	−11.8	−9.4
	% reduction total	−8.1	−0.1	−7.4	−6.0
Test R	$W_{upstream}$	6.8	8.7	10.1	12.5
	$W_{downstream}$	13.8	17.2	20.6	25.1
	W_{total}	20.6	25.9	30.8	37.5
	% reduction upstream	−7.2	1.5	3.6	−0.1
	% reduction downstream	−17.6	−7.1	−7.3	−5.4
	% reduction total	−14.0	−4.1	−3.5	−3.6

3.2. Sediment Motion

Flow-altering countermeasures are designed and built to change the structure of the hydrodynamic pattern, which, in turn, triggers and controls the kinematics of the sediments on the bottom of the scour hole. As a result, the sediment motion pattern is also expected to undergo some modifications if a flow-altering countermeasure is installed. Here, a phenomenological analysis of the mechanisms induced by flow-altering countermeasures was made taking advantage of the measurement of sediment motion described above. Motion patterns were represented by means of the contour lines of time-averaged sediment concentration (as an indicator of sediment activity) and motion lines obtained from the time-averaged sediment velocity (as an indicator of sediment direction). Arguments related to the possibility of time averaging within an evolving process have been provided by Radice et al (2009b) on the basis of the concept of scale separation between the characteristic times used for averaging and those needed for a significant morphologic evolution of the scour hole to occur.

Fig. 5 shows the results obtained for the four experiments and the experimental time $T = 180$ s. The patterns for the upstream region of the hole ($x < 1,000$ mm) were similar for the U and SA cases. For the SB case the motion of sediments presented a significant component along the positive x direction, due to the slot being a way for the sediments to pass through the obstacle. Also in the R case the backward

sediment motion in the region upstream of the abutment nose (x = 950–1, 000 mm; y = 40–100 mm) was almost absent. In this case, since the backward motion of sediments is probably a footprint of the action of the principal vortex, it was concluded that the roughening elements weakened the action of the vortex. The downstream part of the hole presented some differences between various tests, mostly related to the deformation of the recirculation region for the protected tests in comparison with the U test.

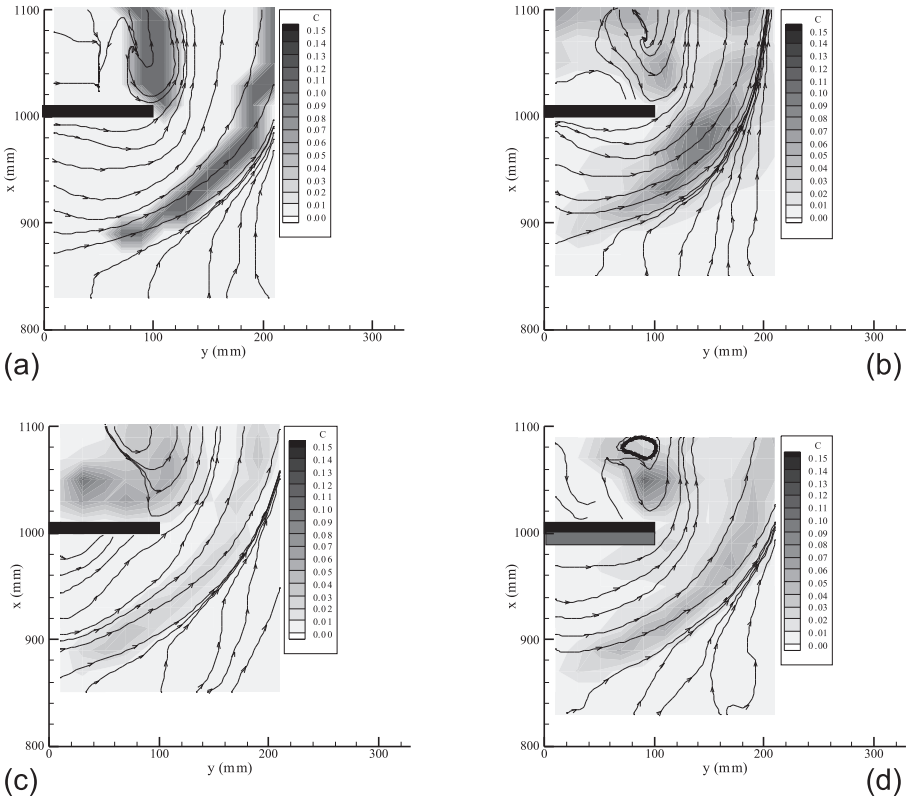

Fig. 5. Spatial distribution of time-averaged sediment concentration (contour lines) and sediment motion lines for experimental time T = 180 s. (a) case U, (b) SA, (c) SB, (d) R

The sediment motion pattern for an intermediate scour stage ($T = 10^3$ s) is depicted in Fig. 6. The U test presented two evident regions of reverse sediment motion: upstream of the abutment nose (x = 950–1, 000 mm, y = 60–100 mm) and for x = 850–900 mm, y = 0–30 mm. These regions were in good agreement with those described by Radice et al (2009b), as a further proof of experiment repeatability. The SA configuration did not present the backward sediment motion in the second region. It was hypothesized above that the scour mitigation induced by the SA configuration

may be related to the interception of the downflow. The results on sediment motion justify a slightly different hypothesis that the slot intercepted the downflow in the left part of the abutment face but not upstream of the abutment nose, where the backward sediment motion was indeed present. The SB case presented features similar to those for the previous experimental time. In the R configuration, the backward sediment motion (and thus the downflow) was not observed upstream of the abutment nose. Interestingly, this change of the flow field at the nose induced a scour reduction at the duct wall. The interpretation of this result is not straightforward; the mutual interaction between scour trends at the two characteristic locations deserves further investigation in the follow-up studies. The findings described here were confirmed by the inspection of the sediment motion pattern for a much evolved scour condition ($T = 4 \times 10^3$ s), shown in Fig. 7.

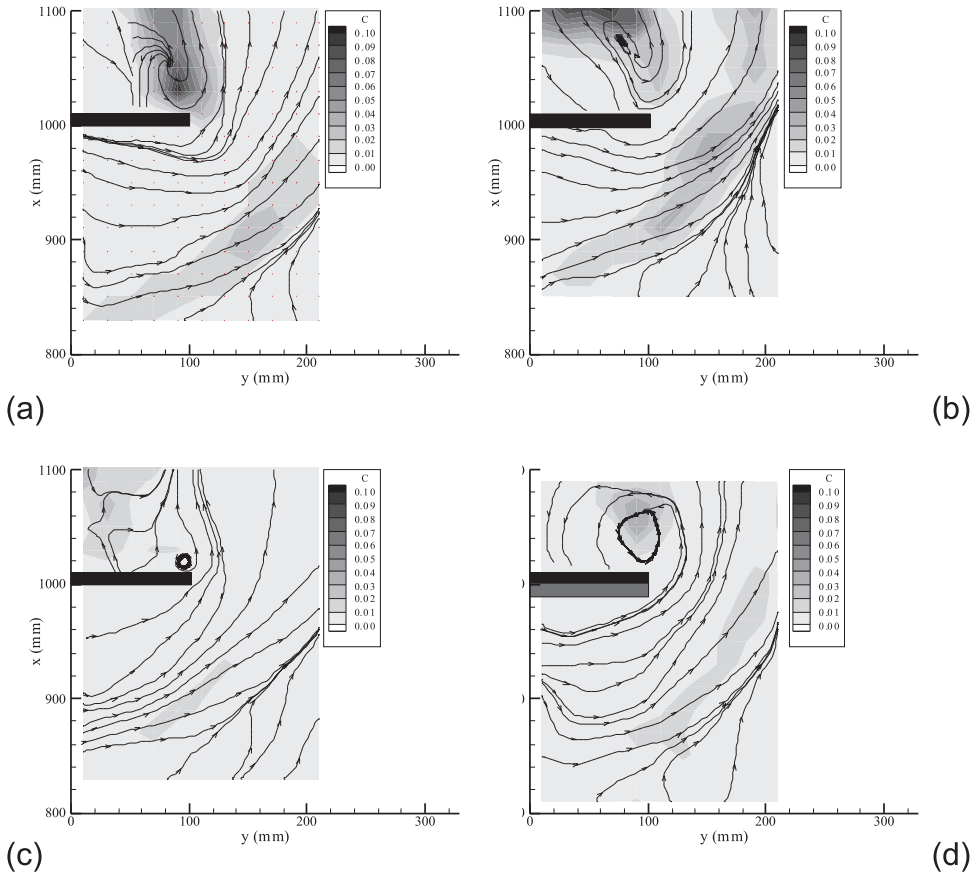

Fig. 6. Spatial distribution of time-averaged sediment concentration (contour lines) and sediment motion lines for experimental time $T = 10^3$ s. (a) case U, (b) SA, (c) SB, (d) R

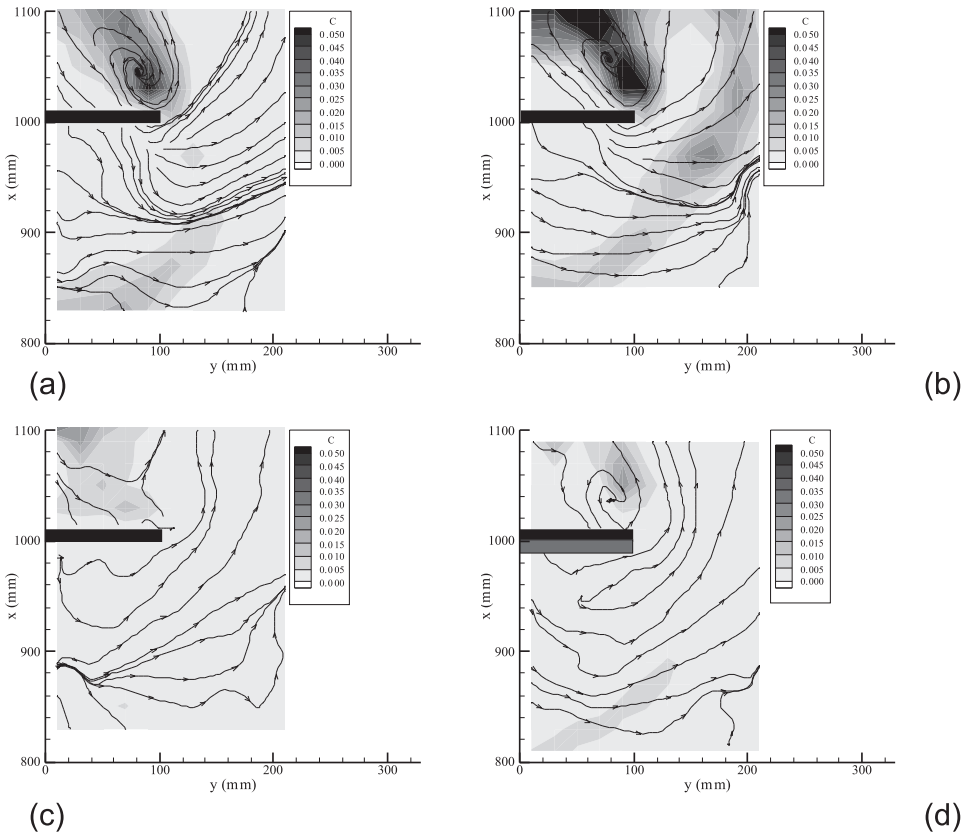

Fig. 7. Spatial distribution of time-averaged sediment concentration (contour lines) and sediment motion lines for experimental time $T = 4 \times 10^3$ s. (a) case U, (b) SA, (c) SB, (d) R

A summary of the above evidence was given as follows. Local scour results from the action of the three-dimensional flow field. Kwan and Melville (1994) reported a general understanding of the process as initiated by the accelerating flow around the structure and developed by the vortex structure. Slots attempt to act on both flow contraction and the downflow. However, it was shown that the downflow was only partially intercepted in the experiments documented here. Roughening elements, though obviously not reducing the contraction ratio, acted as inhibitors of the downflow and also reduced it upstream of the entire abutment face, thus mitigating the scour depth at the wall. The SB configuration was the least effective, since the presence of the slot reduced the distance that the sediments entrained close to the wall had to travel to pass downstream of the abutment. None of the countermeasures managed to inhibit the flow components responsible for scour at the nose.

It is acknowledged that the results proposed in the present study are obviously insufficient for optimal countermeasure design, which should be guided by more ex-

tensive laboratory and field experimentation that was beyond the scope of this work. On the other hand, the analysis presented above shows that it is possible to interpret the performance of scour countermeasures by observing their effect on the sediment motion. This finding might be helpful in devising more extensive experimental campaigns.

4. Conclusions

In this manuscript the use of flow-altering scour countermeasures at vertical-wall abutments was explored. A distinctive feature of the approach was the observation of the phenomenological aspects of the scour process at protected abutments through the analysis of the motion of sediment particles within the scour hole.

A preliminary experimental campaign was run, analyzing the scour process at an unprotected abutment and at abutments protected with slots or roughening elements. The scour reductions obtained were consistent with those documented in the literature for similar conditions. However, the aim of the experiments was not to devise optimal engineering criteria to be used for countermeasure designing, but rather to interpret the working principles of such devices.

The analysis of the sediment motion pattern and of the temporal trend of the scour depth at the abutment nose and in the corner region made it possible to suggest an interpretation of the process. In particular, it was explained how countermeasures such as those tested here may act on flow components. Hypotheses on the working principles based on the measurement of the scour depth could be corroborated or updated by results from the measurement of the sediment motion. The phenomenological indications obtained in this study may be used for guidance in devising extensive experimental campaigns aimed at finding specific technical solutions.

Acknowledgments

The experimental campaign documented here was performed during an internship of the second author at the Politecnico di Milano. Financial support from the Erasmus scholarship fund at Riga Technical University is gratefully acknowledged. This research was also partially supported by the Italian Ministry of University and Research under the PRIN Research Program.

References

Ballio F., Teruzzi A., Radice A. (2009) Constriction effects in clear-water scour at abutments, *Journal of Hydraulic Engineering*, **135** (2), 140–145.

Buffington J. M., Montgomery D. R. (1997) A systematic analysis of eight decades of incipient motion studies, with special reference to gravel-bedded rivers, *Water Resources Research*, **33**, 1993–2029.

Cardoso A. H., Fael C. M. S. (2009) Protecting vertical-wall abutments with riprap mattresses, *Journal of Hydraulic Engineering*, **135** (6), 457–465.

Chiew Y. M. (1992) Scour protection at bridge piers, *Journal of Hydraulic Engineering*, **118** (9), 1260–1269.

Chiew Y. M., Lim S. Y. (2003) Protection of bridge piers using a sacrificial sill, *Proc. Institution of Civil Engineers, Water Maritime and Energy*, **156** (1), 53–62.

Dargahi B. (1990) Controlling mechanism of local scouring, *Journal of Hydraulic Engineering*, **116** (10), 1197–1214.

Dey S., Sumer B. M., Fredsøe J. (2006) Control of scour at vertical circular piles under waves and current, *Journal of Hydraulic Engineering*, **132** (3), 270–279.

Grimaldi C., Gaudio R., Calomino F., Cardoso A. H. (2009) Control of scour at bridge piers by a downstream bed sill, *Journal of Hydraulic Engineering*, **135** (1), 13–21.

Haque M. A., Rahman M., Islam G. M. T., Hussain M. A. (2007) Scour mitigation at bridge piers using sacrificial piles, *International Journal of Sediment Research*, **22** (1), 49–59.

Heidarpour M., Afzalimehr H., Izanidia E. (2010) Reduction of local scour around bridge pier groups using collars, *International Journal of Sediment Research*, **25** (4), 411–422.

Johnson P. A., Hey R. D., Tessier M., Rosgen D. L. (2001) Use of vanes for control of scour at vertical wall abutments, *Journal of Hydraulic Engineering*, **127** (9), 772–778.

Korkut R., Martinez E. J., Morales R., Ettema R., Barkdoll B. (2007) Geobag performance as scour countermeasure for bridge abutments, *Journal of Hydraulic Engineering*, **133** (4), 431–439.

Kumar V., Ranga Raju K. G., Vittal N. (1999) Reduction of local scour around bridge piers using slots and collars, *Journal of Hydraulic Engineering*, **125** (12), 1302–1305.

Kwan R. T. F., Melville B. W. (1994) Local scour and flow measurements at bridge abutments, *Journal of Hydraulic Research*, **32** (5), 661–673.

Lagasse P. F., Zevenbergen L. W., Schall J. D., Clopper P. E. (2001) *Bridge scour and stream instability countermeasures*, Federal Highway Administration, FHWA NHI 01-003, HEC-23.

Li H., Barkdoll B. D., Kuhnle R., Alonso C. (2006) Parallel walls as an abutment scour countermeasure, *Journal of Hydraulic Engineering*, **132** (5), 510–520.

Mashahir M. B., Zarrati A. R., Mokallaf E. (2010) Application of riprap and collar to prevent scouring around rectangular bridge piers, *Journal of Hydraulic Engineering*, **136** (3), 183–187.

Melville B. W., Coleman S. E. (2000) *Bridge scour*, Water Resources Publications: Highlands Ranch, Colorado, USA.

Melville B. W., Hadfield A. C. (1999) Use of sacrificial piles as pier scour countermeasures, *Journal of Hydraulic Engineering*, **125** (11), 1221–1224.

Melville B. W., van Ballegooy S., Coleman S., Barkdoll B. (2006a) Countermeasure toe protection at spill-through abutments, *Journal of Hydraulic Engineering*, **132** (3), 235–245.

Melville B. W., van Ballegooy S., Coleman S., Barkdoll B. (2006b) Scour countermeasures for wing-wall abutments, *Journal of Hydraulic Engineering*, **132** (6), 563–574.

Meyer-Peter E., Müller R. (1948) Formulas for bed-load transport, *Proc. of the II Meeting of IAHR*, Stockholm, Sweden.

Radice A. (2010) Discussion of "Protecting vertical-wall abutments with riprap mattresses" by A.H. Cardoso and C.M.S. Fael, *Journal of Hydraulic Engineering*, **136** (10), 848–849.

Radice A., Ballio F. (2008) Double-average characteristics of sediment motion in one-dimensional bed load, *Acta Geophysica*, **56** (3), 654–668.

Radice A., Ballio F., Porta G. (2009a) Local scour at a trapezoidal abutment: Sediment motion pattern, *Journal of Hydraulic Research*, **47** (2), 250-262.

Radice A., Ballio F., Tran C. K. (2010) Gravity- and turbulence-dominated sediment motion in the clear-water scour process at a vertical-wall abutment in pressurized flow, *Archives of Hydro-Engineering and Environmental Mechanics*, **57** (1–2), 3–19.

Radice A., Malavasi S., Ballio F. (2006) Solid transport measurements through image processing, *Experiments in Fluids*, **41**, 721–734.

Radice A., Porta G., Franzetti S. (2009b) Analysis of the time-averaged properties of sediment motion in a local scour process, *Water Resources Research*, **45**, W03401.

Shields A. (1936) Anwendung der Aehnlichkeitsmechanik und der Turbulenz Forschung auf die Geschiebebewegung, *Mitt. der Preussische Versuchanstalt für Wasserbau und Schiffbau*, Tech. Hochsch., Berlin, Germany, 26.

Sui J., Afzalimehr H., Samani A. K., Maherani M. (2010) Clear-water scour around semi-elliptical abutments with armored beds, *International Journal of Sediment Research*, **25** (3), 233–245.

Vittal N., Kothyari U. C., Haghighat M. (1994) Clear-water scour around bridge pier group, *Journal of Hydraulic Engineering*, **120** (11), 1309–1318.

Zarrati A. R., Chamani M. R., Shafaie A., Latifi M. (2010) Scour countermeasures for cylindrical pier using riprap and combination of collar and riprap, *International Journal of Sediment Research*, **25** (3), 313–321.

Zarrati A. R., Gholami H., Mashahir M. B. (2004) Application of collar to control scouring around rectangular bridge piers, *Journal of Hydraulic Research*, **42** (1), 97–103.